Article
Chinese Science Bulletin
SPECIAL TOPIC
Geological Processes in Carbon Cycle
December 2011 Vol.56 No.35: 3766–3773
doi: 10.1007/s11434-011-4377-3

Preliminary regional estimation of carbon sink flux by carbonate rock corrosion: A case study of the Pearl River Basin

CAO JianHua[1,2*], YANG Hui[1,2,3] & KANG ZhiQiang[1,2,4]

[1] *Institute of Karst Geology, Chinese Academy of Geological Sciences/Key Laboratory of Karst Dynamics of Ministry of Land and Resources, Guilin 541004, China;*
[2] *International Research Center on Karst (IRCK) Under the Auspices of UNESCO, Guilin 541004, China;*
[3] *Graduate University of Chinese Academy of Sciences, Beijing 100049, China;*
[4] *School of Environmental Studies, China University of Geosciences (Wuhan), Wuhan 430074, China*

Received July 5, 2010; accepted December 2, 2010; published online April 13, 2011

The formation of carbonate rocks has had a dramatic sink effect on atmospheric CO_2 throughout geological time. The wide global distribution of carbonate rocks and their strong sensitivity to climate change mean that carbonate rock corrosion consuming air/soil CO_2 can play an important role in the global carbon cycle. The carbon sink accounts for 12.00%–35.29% of the "missing carbon" in the global carbon cycle. Using the Pearl River Basin as a case study, we analyzed comprehensively the factors impacting karstification and the carbon sink, collected existing monitoring data, and established a regression equation incorporating corrosion rate, annual precipitation, soil respiration rate and net primary productivity from typical observation sites. We used Arcview 3.3 software to estimate spatially the atmospheric CO_2 sink flux in the Basin's karst region by combining the distribution of carbonate rock categories. We determined annual CO_2 consumption due to carbonate rock corrosion to be 1.54×10^7 t $CaCO_3$ a^{-1}, equal to 1.85×10^6 t C a^{-1}.

Pearl River Basin, carbonate rock corrosion, carbon sink

Citation: Cao J H, Yang H, Kang Z Q. Preliminary regional estimation of carbon sink flux by carbonate rock corrosion: A case study of the Pearl River Basin. Chinese Sci Bull, 2011, 56: 3766–3773, doi: 10.1007/s11434-011-4377-3

The lithosphere is the largest carbon reservoir in the Earth System. Carbon stored in carbonate rocks is estimated at more than 6.0×10^{16} t C, as much as 1562 times the total ocean carbon quantity and 3.0×10^4 times that in terrestrial vegetation [1]. The formation of carbonate rocks has accordingly had a dramatic sink effect on atmospheric CO_2 throughout geological time [2]. Carbonate rocks cover ~15% of the global land surface, or ~22×10^6 km^2 [3]. The karst area in China is ~3.4×10^6 km^2, accounting for ~15.6% of the global karst area [4]. Since the launch of the IGCP379 program "Karst Processes and the Carbon Cycle (1995–1999)" [5], the study of carbon sink effects by karstification has received wide attention from researchers around the world. The annual flux of atmospheric CO_2 uptake by global karstification has been estimated using different approaches, which have yielded differing results. For example, the estimation of annual flux by Yuan et al. [6] was 0.6 Gt C a^{-1} and 0.3 Gt C a^{-1} by Philippe [7]. There is a so-called missing carbon sink in the global carbon cycle, with an estimated mass of 1.7–2.5 Pg C a^{-1} [8]. Thus, the carbon-sink flux of global karstification ranges potentially from 12.00% to 35.29% of the missing carbon sink, and has become a focus of global carbon cycle research.

Using the Pearl River Basin as a case study, we used data from typical monitoring sites to estimate the regional carbon-sink flux in karst areas, and developed extrapolation approaches from sites' data to the entire area. We analyzed comprehensively the factors impacting karstification and the carbon sink, collected existing data, and established a regression equation using corrosion rate, annual precipitation,

*Corresponding author (email: jhcao@karst.edu.cn)

soil respiration rate and net primary productivity (NPP) at typical observation sites. We used Arcview3.3 software to estimate spatially the atmospheric CO_2 sink flux in the Basin's karst regions by combining the distribution of different carbonate rock categories.

1 The study area

The Pearl River Basin is located in the humid subtropical region of south China (102°15′ –115°35′E, 21°50′–26°48′N). The Basin lies within the provinces of Yunnan, Guizhou, Guangxi and Guangdong, and has a drainage area of 452600 km^2, which accounts for 4.71% of China's total land area [9,10]. The karst area in the Basin is 158440 km^2, accounting for around 35.0% of total Basin area [9]. The provinces mentioned above all have large distributions of carbonate rocks: in Yunnan Province, carbonate rocks Precambrian to Tertiary outcrop with an area of 31300 km^2, excepting of Jurassic, Cretaceous; in Guizhou Province Cambrian, Devonian and Triassic rocks outcrop with an area of 33900 km^2; in Guangxi Zhuang Autonomous Region Devonian to lower Triassic carbonate rocks outcrop with an area of 78000 km^2; and in Guangdong Province carbonate rocks are distributed in the up stream of the Beijiang River, down stream of the Lianjiang River and the Xijiang River, and the western Guangdong, with a total outcrop area of 7600 km^2.

2 Karst processes and factors influencing the karst carbon sink

2.1 Karst processes

Karst processes include the corrosion and deposition of carbonate rocks:

The corrosion of carbonate rock is the process of CO_2 uptake and consumption, which is expressed as follows [11]:

For limestone:

$$CaCO_{3(solid)}+CO_{2(gas)}+H_2O_{(liquid)} \Leftrightarrow Ca^{2+}_{(liquid)}+2HCO^{-}_{3(liquid)} \quad (1)$$

For dolomite:

$$CaMg(CO_3)_{2(solid)}+2CO_{2(gas)}+2\ H_2O_{(liquid)} \Leftrightarrow Ca^{2+}_{(liquid)}+Mg^{2+}_{(liquid)}+4HCO^{-}_{3(liquid)} \quad (2)$$

In bare carbonate rock areas the CO_2 originates directly from the atmosphere, whereas in vegetation- and soil-covered areas it comes mainly from the soil processes. For limestone, 1 mol $CaCO_3$ corrosion corresponds to 1 mol CO_2 uptake from air. For dolomite, 1 mol $CaMg(CO_3)_2$ corrosion corresponds to 2 mol CO_2 uptake from air.

Changes in temperature, pressure and hydrodynamic conditions may cause carbonate precipitation and sedimentation in saturated and supersaturated waters, which releases CO_2. The subsequent carbonate rock deposits ultimately record climate change information stored in cave stalagmites and travertine. Therefore, the karst corrosion reactions described above are reversible. However, the focus of this paper is the major factors contributing to carbonate rock corrosion and influencing the carbon sink.

2.2 Factors influencing the karst carbon sink

(i) Temperature and precipitation. The most important factor in carbonate rocks corrosion is precipitation, which influences directly hydrological conditions and runoff. Many existing mathematical models that describe carbonate rock corrosion, directly use precipitation or runoff as variable, (s). For example, Sweeting [12] established a formula correlating the corrosion rate (D_R) of carbonate rocks and precipitation (P):

$$D_R=0.0043P^{1.26}.$$

Based on the statistical data collected from 232 drainage basins in France, Amiotte and Probst [13] established a formula reflecting atmospheric CO_2 consumption by rock corrosion:

$$F_{CO_2} = a \cdot Q,$$

where F_{CO_2} is CO_2 consumption (10^{-3} mol km^{-2}), Q is the surface runoff, L km^{-2} s^{-1} and a is the coefficient of different rock types.

Liu [11] demonstrated a linear correlation between carbonate rock corrosion rate (D_R) and runoff (P–E):

$$D_R=0.0544\ (P–E)–0.0215\ (r^2=0.98),$$

where P is precipitation (mm), and E is evaporation (mm).

Jiang et al. [14] found that the karst area in Guilin, China is the largest carbon sink per unit area because of CO_2 uptake resulting from high regional precipitation. The arid Golmud region has the smallest carbon sink because of low precipitation.

The influence of temperature on carbonate rocks corrosion is relatively complex. To a great extent, temperature influences the CO_2 concentration and migration rate in the karst systems through biological processes. At low temperatures, biological processes and carbon migration are weak, which is good for the stability and migration of CO_2 in water. In contrast, at high temperatures biological processes and carbon migration are vigorous, which reduces the stability of CO_2 in water. A semi-closed static corrosion experiment conducted by Huang et al. [15] showed that temperatures ranging from 25 to 60°C provide the best corrosion conditions, with lower and higher temperatures being unfavorable. Pulina [16] showed a correlation between carbonate rock corrosion rate, temperature and precipitation: at lower temperatures (–5 to 5°C) the variation of precipitation has only slight impacts on corrosion rate, whereas at

relatively higher temperatures (16 to 20°C) the corrosion rate increases rapidly with increasing precipitation.

(ii) Hydrodynamics and hydrochemistry. The corrosion of carbonate rocks is a water-rock interaction. A diffusion boundary layer (DBL) exists at the solid carbonate rock/water interface [11]. With increasing flow rate, the DBL becomes thinner and the carbonate rock corrosion rate increases.

Runoff that passes through terrain composed of clastic sediments and then enters karst terrain is allogenic water with lower hardness and pH value than water passing solely through karst, and more aggressively weathers carbonate rocks. Liu [17] conducted quantitative research on the corrosion kinetics of allogenic water in Yaoshan, Guilin. The results showed that the limestone corrosion rate in allogenic water is 1000–1500 mm ka^{-1}, which is 10–15 times higher than that in karst water. The corrosion rate of limestone in streams with a flow rate of 20 cm s^{-1} or 60 cm s^{-1} is 2 or 3 times higher than that in static water.

(iii) Biological factors. The biosphere exchanges and transfers mass and energy with other spheres so as to penetrate the entire Earth Surface System [18,19]. Of which organisms are the most active geological agent [20]. With CO_2 as the central link, biological action connects biospheric carbon with the dynamic triphase CO_2–H_2O–$CaCO_3$ open disequilibrium karst dynamic system. Organisms have a strong stimulative effect on corrosion of carbonate rocks, which is caused mainly by high-concentration soil CO_2 with and erosional secretions produced by plants and microorganism metabolism. Data collected in field experimental research show that subsoil corrosion of carbonate rocks is far higher than of those exposed to air, because CO_2-concentration in soil is scores or hundreds of times higher than that in the atmosphere.

The results of simulations conducted by Cao et al. [21] showed that under different vegetation, the differences in biological activity lead to the difference in corrosion rate. The corrosion rate of the tree-soil-limestone system with an extensive root system was 3.84 and 2.36 times those of a soil-limestone system and herb-soil-limestone system, respectively. Jennings [22] established a correlation between the corrosion rate and annual average runoff in different countries to show that the soil-vegetation system increases carbonate rocks corrosion.

Taking into account the influence of the above factors on karstification and the carbon sink, we selected the following to be the variables for estimating carbon sink flux in the Pearl River Basin:

Precipitation: the main agent of karstification and carbon migration;

Soil respiration: CO_2 concentration and dynamics in the soil environment greatly promote karstification;

Net primary productivity (NPP) of vegetation: Different vegetation succession stages affect carbon cycle intensity, which influences karstification and the carbon sink;

Lithology of carbonate rocks: the differences in mineral components (e.g. dolomite or calcite) and the content of acid non-soluble substances within carbonate rocks can cause two-fold or three-fold difference in the corrosion rate under the same precipitation and vegetation conditions.

Because temperature influences CO_2 concentration and transport rate in karst systems via biological actions, and the detailed processes of temperature in carbonate rock corrosion are relatively complicated, to a certain extent soil and vegetation may substitute temperature. Thus, we do not involve temperature as a variable in this analysis. Nor do we involve hydrodynamic factors or hydrochemistry because of a lack of sufficient data.

3 Methods and data sources

3.1 Methods

We collected relevant data on precipitation, vegetation net primary productivity, soil respiration and types of carbonate rocks to create a regression equation that describes carbonate corrosion rate at typical monitoring sites. Using the regression equation, we analyzed the lithology and purity of the carbonate rocks, and then estimated the spatial distribution of carbonate rock corrosion rate in the study area to calculate the annual carbon sink flux by karstification. The carbon sink flux was estimated as:

$$F_{CO_2} = r \cdot s \cdot a\, M_1(CO_2)/M_2(CaCO_2), \quad (3)$$

where F_{CO_2} is CO_2 sink (10^9 g a^{-1}), r is the corrosion rate of limestone tablets (g cm^{-2} a^{-1}), a is the specific weatherability of carbonate rocks, s is the area of carbonate rocks (km^2), $M_1(CO_2)$ is the molecular weight of CO_2 (44), and $M_2(CaCO_3)$ is the molecular weight of a standard pure limestone sample with acid-insoluble matter <1% from the Devonian Rongxian Group ($CaCO_3$ (100)).

3.2 Data sources

The vector-graph of the Pearl River Basin was provided by the Pearl River Water Resources Commission. Precipitation data and the NPP raster data came from the Institute of Geographic Sciences and Natural Resources Research, CAS (Beijing CASW Data Technology Co., Ltd.). Soil respiration raster data came from the Data Sharing Infrastructure of Earth System Science of the Institute of Geographic Sciences and Natural Resources Research, CAS.

Lithology and carbonate rock type came from the 1:500000 geological vectorgraph provided by the University of Geosciences (Wuhan). Based on the strata description, we developed a carbonate rock type map (Figure 1). The lithology of carbonate rocks, type classification and conversion method are presented in [23] and [24]. Their area distributions are listed in Table 1.

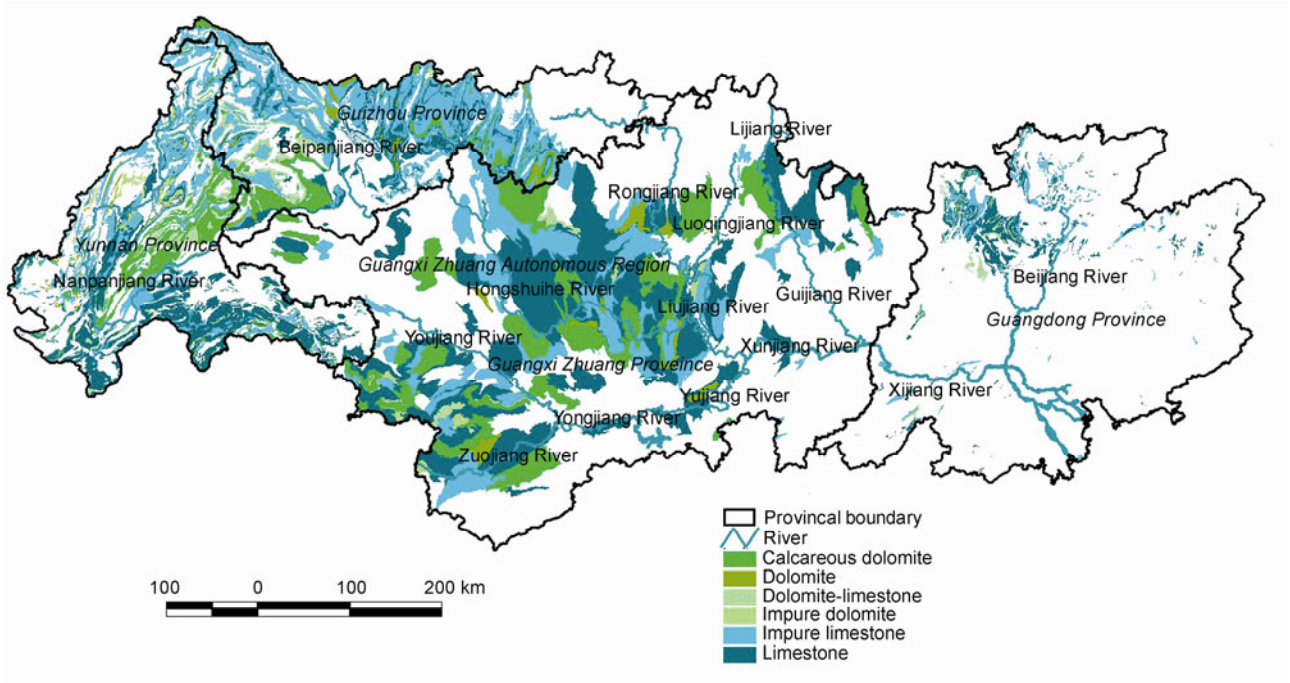

Figure 1 Distribution of different categories of carbonate rocks in the Pearl River Basin.

Table 1 Distribution area statistics of carbonate rock categories in the Pearl River Basin

Carbonate rock type	Area (km^2)	Proportion of Pearl River Basin (%)
Dolomite	4238.47	2.68
Dolomitic limestone	6604.49	4.17
Impure dolomite	2509.31	1.58
Impure limestone	51346.28	32.41
Limestone	63198.02	39.89
Calcareous dolomite	30543.74	19.28
Total amount	158440.31	100

4 Results

4.1 Establishment of the regression equation governing carbonate corrosion rate and impact factors

Based on 57 sets of limestone corrosion rates in the study area [25–27] and a corresponding raster chart obtained from the geographic coordinates, the corresponding precipitation, the soil respiration rate (Sr) and NPP were obtained (Table 2). The raster chart was made using annual averages for many years, whereas the carbonate corrosion rate corresponded with the precipitation of a specific year. Therefore, the corrosion rates were modified appropriately.

These data are of different dimensions. To ensure their comparability, we did the data processing with dimensionless normalization. According to the principle of least squares, we conducted regression analysis on the first power, second power, third power, fourth power and fifth power of the processed data using SPSS13.0 software, and obtained regressive R^2, Adjusted R^2 and P values corresponding to each factor. The optimum regression equation was obtained with the fourth power data, and the significance levels corresponding with each factor were P=0.0003 for Pa, P=0.0000 for Rs and P=0.0021 for NPP. Hence the regression equation governing the correlation between carbonate corrosion rate (Dr), annual average precipitation (Pa), soil precipitation (Rs) and net primary productivity (NPP) was established as

$$\mathrm{Dr}=0.176+0.696\times \mathrm{Pa}^4+0.483\times \mathrm{Rs}^4+0.324\times \mathrm{NPP}^4$$
$$(R^2=0.728,\ P<0.01). \quad (4)$$

4.2 Production of the karst corrosion rate map

Based on the above equation, the annual average precipitation in the study area, soil respiration raster chart and NPP raster chart were calculated into a karst corrosion rate raster chart (unit: g $CaCO_3$ m^{-2} a^{-1}) using Arcview3.3 (Figure 2). The maximum, minimum and mean corrosion rates in the study area were 162.31, 77.82 and 115.24 g $CaCO_3$ m^{-2} a^{-1}, respectively. The calculated mean corrosion rate was approximately two times higher than the rate of 65.789 g $CaCO_3$ m^{-2} a^{-1} calculated by Yao [28], and slightly less than the annual denudation rate of 155.52 g $CaCO_3$ m^{-2} a^{-1}. In view of the annual carbonate rock corrosion rate 57.6 mm ka^{-1} calculated by Liu [11] with the DBL model, we calculated the above-mentioned annual denudation rate of carbonate rocks with the average density of carbonate rocks (2.7 g cm^{-3}). The estimation of the corrosion rate 115.24 g $CaCO_3$ m^{-2} a^{-1} here lies between the above two calculation

Table 2 Carbonate rock corrosion rate and corresponding impact factors at typical monitoring sites in the Pearl River Basin

	Location	Corrosion rate (mm ka^{-1})	Precipitation (mm)	Soil respiration (g C m^{-2} a^{-1})	NPP (g C m^{-2})
Yunnan	Mengzi*	41.1	1058	1179.2	316.5
	Mile*	30.0	884	1365.8	44.8
	Qujing*	45.0	1030	1352.4	190.0
	Luoping*	65.0	1492	1498.1	202.8
	Fuyuan*	50.2	1332	1446.2	190.4
	Lunan	32.0	932	1344.1	219.6
	Tonghai*	30.0	880	1339.6	196.3
Guizhou	Libo	65.5	1194	309.4	1116.2
	Qinglong*	55.0	1407	1445.8	268.3
	Anlong*	60.0	1260	1502.5	203.7
	Ziyun*	51.1	1203	1487.5	194.5
	Guanling*	49.8	1342	1496.6	208.4
	Zhenfeng*	70.0	1290	1527.4	229.6
	Luodian*	55.0	1182	1605.7	222.6
	Guiyang	44.5	1112	1398.1	248.2
	Wuchuan	36.1	1094	1438.1	245
Guangxi	Huanjiang	59.1	1338	911.5	313.3
	Yongfu*	60.0	1702	1759.9	498.1
	Yishan*	55.0	1321	1733.9	304.4
	Liucheng*	55.0	1372	1733.5	421.5
	Tian'e*	56.0	1362	1745.5	398.8
	Du'an*	50.0	1377	1721.4	226.9
	Longlin*	80.0	1496	1814.5	264.7
	Mashan*	70.0	1158	1577.6	297.1
	Shanglin*	80.0	1542	1842.1	344.5
	Luzhai*	65.0	1559	1845.8	365.7
	Xincheng*	54.0	1481	1747.8	474.7
	Gongcheng*	60.3	1379	1778.9	283.9
	Rong'an*	59.8	1452	1718.6	470.4
	Rongshui*	70.4	1622	1755.3	455.5
	Nandan*	69.7	1438	1671.9	422.5
	Guilin	50.2	1355	1708.9	211.8
	Yaji	89.7	1703	1753.3	383.0
	Yaji	115.1	2765	1704.0	597.7
	Yaji	39.1	1585	318.3	1766.4
	Yaji	74.2	2024	298.0	1837.8
	Yaji	104.7	2659	308.3	1854.6
	Yaji	93.4	2266	338.4	1848.0
	Yaji	32.2	1424	331.1	1701.1
	Yaji	85.2	2106	354.7	1820.2
	Yaji	72.9	1950	291.2	1803.2
	Yaji	89.4	2143	354.1	1895.6
	Yaji	85.9	2018	339.3	1861.9
	Yaji	38.7	1595	321.2	1748.4
	Yaji	56.8	1388	331.4	1716.0
	Maocun	74.6	1547	1674.0	537.7
Beijing	Xishan	22.0	528	734.8	225.9
	Xishan	29.0	702	968.0	374.4
	Xishan	27.6	759	424.9	582.6
Chongqing	Qingmuguan	44.7	1008	556.8	664.8
	Qingmuguan	32.2	1180	795.2	398.6
	Qingmuguan	26.3	1092	986.0	212.1
	Qingmuguan	21.4	1038	1509.6	601.2
	Qingmuguan	24.2	1004	742.0	208.2
	Nanchuan	62.5	940	2290.4	592.7
	Nanchuan	27.9	845	565.7	367.0
	Nanchuan	26.8	982	1261.2	219.2

* Data from [25–27]. The rest are field survey data from 1991 to 2009, with values presented the arithmetic mean of the year.

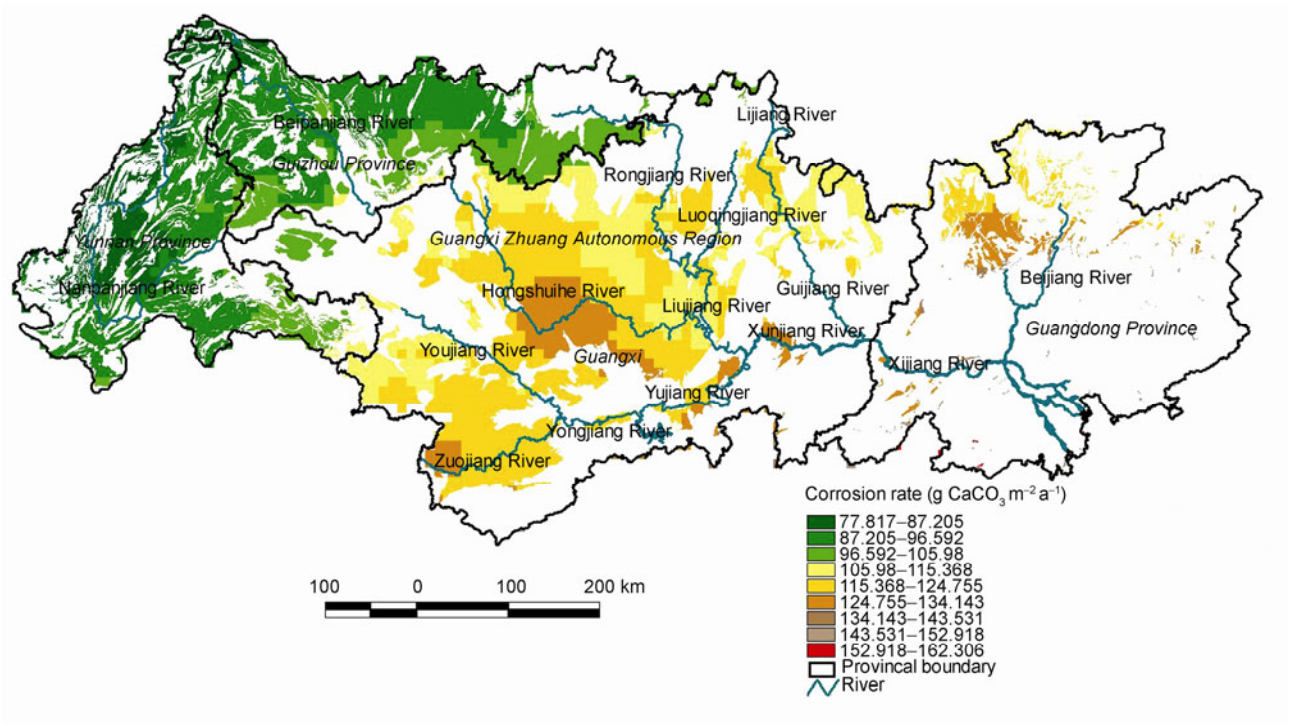

Figure 2 Corrosion rate distribution in karst areas of the Pearl River Basin.

results (65.789 g $CaCO_3$ m^{-2} a^{-1} and 155.52 g $CaCO_3$ m^{-2} a^{-1}).

4.3 Estimation of karstification carbon sink flux

The carbon sink flux caused by karstification varies with the category and purity of carbonate rocks. Our calculated corrosion rate needs to be rectified according to the different types of carbonate rocks in the Pearl River Basin. Other research showed that the carbonate rock corrosion rate increases with the content of calcite (positive correlation) and decreases with the content of dolomite (negative correlation) [29,30]. When estimating the carbon sink flux caused by corrosion of carbonate rocks, the specific corrosion of different rock types can be regarded as the coefficient of lithology.

Using the mapped carbonate rock areas with the corresponding specific corrosion rates [29–31], we estimated the annual carbonate rock corrosion rate of various categories with formula (3) and converted it into the amount of CO_2 consumption, namely the carbon sink flux caused by karstification (Figure 3). The atmospheric CO_2 sink flux contributed by karstification is 1.54×10^7 t $CaCO_3$ a^{-1}, equaling a pure carbon flux of 1.85×10^6 t C a^{-1} (Table 3). The results of this study were comparable with previous results [32]: (1) Wei used DIC concentration multiplied by flow, and then by integrating time of hydrological year 2000–2001, then obtained a total DIC's output capacity of 5.50×10^6 t C a^{-1} in the Pearl River; and (2) Gao used DIC concentration multiplied by flow, and then by integrating time of hydrological year 1997–1998, obtained a total DIC's output capacity of 7.01×10^6 t C a^{-1} in the Pearl River. Our result is lower than the two. The possible reasons for that may be (1) only karst area was calculated in this study, the karst area occupies 35% in total area of the Pearl River Basin; and (2) the factor of hydraulic impacts was ignored.

5 Discussion and prospects

5.1 Compared with other rocks types, karst processes (mainly corrosion of carbonate rocks) have a more significant sink effect on atmospheric CO_2

The wide global distribution of carbonate rocks makes the karst terrain an important component of the Earth Surface System. The corrosion of carbonate rocks causes rapid consumption of atmospheric CO_2, and leads to a significant sink effect on atmospheric CO_2 by terrestrial corrosion which in turn affects global climate. With the GEM-CO_2 model put forward by the IGCP404, the carbon sink flux by rock corrosion in mainland of China is calculated to be 1.41×10^7 t C a^{-1}, and the consumed atmospheric CO_2 flux contributed by carbonate rock corrosion may be 0.74×10^7 t C a^{-1}, accounting for 52.65% of the total carbon sink flux [28]. The contribution of carbonate rock corrosion to HCO_3^- formation and corresponding cations in lakes and rivers around the world is 38% [33].

5.2 Future exploration of the processes and mechanisms of the karstification carbon sink

Because the main existing form of the karstification carbon

Table 3 Estimation of carbon sink flux by karstification in the Pearl River Basin

Lithology	Area (km^2)	Specific corrodibility	Annual corrosion (t $CaCO_3$ a^{-1})	Carbon equivalent (t Ca^{-1})
Dolomite	4238.47	0.505	246676.23	29601.15
Dolomitic limestone	6604.49	0.833	633997.49	76079.70
Impure dolomite	2509.31	0.767	221795.60	26615.47
Impure limestone	51346.28	0.767	4536675.31	544401.04
Limestone	63198.02	0.965	7028036.93	843364.43
Calcareous dolomite	30543.74	0.770	2710292.66	325235.12
Total amount	158440.31		15377474.22	1845296.91

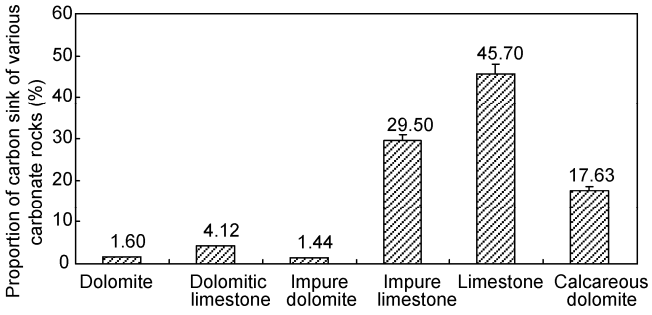

Figure 3 Proportion of karstification carbon sink flux caused by different carbonate rocks in the Pearl River Basin.

sink is DIC (HCO_3^-), which in certain conditions can change into CO_3^{2-} with CO_2 release, many scholars in China and abroad have doubted the existence and effect of the karstification sink. Some research findings show that the annual CO_2 uptake from the global water cycle is ~0.8×10^9 t C, accounting for ~10.1% of CO_2 emitted by human activities. The uptake increases with the corrosion of carbonate rocks and dissolved CO_2 consumption by aquatic plant photosynthesis [34]. Thus, three aspects of the formation of carbon sink by karstification need to be further researched: (1) the existing form, transformation and stability of the karst carbon sink in water; (2) the influence of hydrodynamics, hydrochemistry and biological action in water on the stability and migration of the karst carbon sink [35]; and (3) the sink effect of carbonate lithosphere in response to atmospheric CO_2, the feedbacks among lithosphere, atmosphere, hydrosphere and biosphere, and the tracing of the karst carbon sink in the Earth Surface System.

5.3 Further improvement of the karst carbon sink flux estimation model

We estimated a regional karstification carbon-sink flux by analysis of major causative factors. Our estimates were close to previous results conducted with different estimation methods, suggesting the feasibility and reliability of our approach. Nevertheless, our analysis has three clear deficiencies in the regression equation: (1) hydrodynamics was not accounted for in the calculation. The Pearl River originates in Maxiong Hill of the Wumeng Mountain Range in Qujing, Yunnan Province, with a highest altitude of 2853 m and a length of 2214 km. Sea level is the base level of the river. The average slope gradient of the river is larger than 1.23‰. Such dramatic hydrodynamic conditions should promote the corrosion rate and intensity of carbonate rocks; (2) hydrochemical processes were neglected. Allogenic water with a strong corrosion effect can enhance carbonate rock corrosion. The effect of allogenic water can be regarded as a prolonged corrosion of carbonate rocks by precipitation to improve and strengthen the carbon-sink flux by karstification; and (3) the estimation model employed in this paper is a mathematical regression equation. Although we used various factors that impact the karst carbon sink, research on the correlation between single factors and carbon sink flux caused by corrosion needs to be furthered, and the estimation methods for quantifying karstification carbon-sink flux need to be further improved.

We thank three anonymous referees for their constructive suggestions and Lu Qian from Institute of Karst Geology (IKG), Chinese Academy of Geological Sciences (CAGS) and an anonymous editor for help with English revision. This work was supported by the National Natural Science Foundation of China (40872213), the Project of the China Geological Survey (1212010911062) and the Project of the China Geological Survey(S-2010-KP03-07-02).

1 Falkowski P, Scholes R J, Boyle E, et al. The global carbon cycle: A test of our knowledge of Earth as a system. Science, 2000, 290: 291–296
2 Fairbridge R W. Carbonate rock and paleoclimate. In: Advance in Sedimentology-Carbonate Rock. Beijing: Petroleum Chemical Industry Press, 1978. 232–255
3 Yuan D X. Modern karstology and global change study (in Chinese). Earth Sci Fronti 1997, 4: 17–25
4 Yuan D X. Karst of China (in Chinese). Beijing: Geological Publishing House, 1991
5 Yuan D X. The carbon cycle in karst. Z Geomorph N F, 1997, 108: 91–102
6 Yuan D X. Zhang C. Karst Processes and the Carbon Cycle, Final Report of IGCP379 (in Chinese). Beijing: Geological Publishing House, 2002
7 Philippe G. Role of karstic corrosion in global carbon cycle. Glob Planet Change, 2002, 33: 177–184
8 Lal R. Carbon sequestration. Phil Trans R Soc B, 2008, 363: 815–830
9 Huang J X, Lin T J. Basic characteristics of karst groundwater in the Pearl River Basin (in Chinese). Pearl River, 1983: 12–15
10 Wang Z L, Chen X H. Net primary productivity and its spatio-temporal patterns in the Pearl River Basin. Acta Sci Nat Univ Sunyatseni, 2006, 45: 106–110

11 Liu Z H. Contribution of carbonate rock weathering to the atmospheric CO_2 sink. Carsol Sin, 2000, 19: 293–300
12 Sweeting M M. Karst Landforms. London: MacMillan Press Ltd., 1972
13 Amiotte S P Probst J L. Flux de CO_2 consommé par altération chimique continentale: Influences du drainage et de la lithologie. C R. Acad Sci Paris, 1993, 317: 615–622
14 Jiang Z C, Jiang X Z, Lei M T. Estimation of atmospheric CO_2 sink of karst areas in China based on GIS and limestone tablet loss data (in Chinese). Carsol Sin, 2000, 19: 212–217
15 Huang S Y, Song H R. The Corrosion of carbonates and environment temperature (in Chinese). Carsol Sin, 1987, 6: 287–293
16 Pulina M. Preliminary studies on denudation in SW Spitsbergen. Bull l'Acad Polon Sci, Serie Sci Terre, 1974, 22: 2–3
17 Liu Z H. Field experimental research on the corrosion kinetics of limestone and dolomite in allogenic water—Case from Yaoshan Mt. Guilin (in Chinese). Carsol Sin, 2000, 19: 1–4
18 Golubic S. Carbonate corrosion. The Biology of Cyanobacteria. Oxford: Oxford Blackwell Scientific Publications Ltd, 1978. 107–129
19 Zhang Y. A new outlook on the earth (in Chinese). Adv Earth Sci, 1992, 7: 57–64
20 Yin H F, Xie S C, Zhou X G. Advances and trends on the study of microbial metallogenesis (in Chinese). Earth Sci Front, 1994, 1: 148–156
21 Cao J H, Yuan D X, Pan G X, et al. Influence of soil carbon transfer under different vegetation on carbon cycle of karst dynamics system (in Chinese). Earth Environ, 2004, 32: 90–96
22 Jennings J N. Karst Geomorphology. London: Oxford Basil Blackwell Ltd., 1985
23 Karst Research Group of the Institute of Geology, Chinese Academy of Geology Sciences. Study on Karst of China. Beijing: Science Press, 1979
24 Wang Y, Li Y, Tan J Z, et al. Occurrence of Karst Water in Fault Basins (in Chinese). Kunming: Yunnan Science and Technology Press, 2003
25 Cao J H, Jiang Z C, Yang D S, et al. Soil loss tolerance and prevention and measurement of karst area in southwest China (in Chinese). Soil Water Conser Chin, 2008, 40–45
26 Fang J F, Lin J S, Li J Z, et al. Relation of solution to environment in karst area—A case study of Hongshui River Basin (in Chinese). Acta Geogr Sin, 1993, 48: 122–130
27 Zhu M Q, Cao J H, Guo F, Analysis on the carbon amounts originated by the weathering of Carbonate rocks and the influence of soils on the carbon turnover process in karst areas (in Chinese). Carsol Sin, 2007, 26: 202–206
28 Yao R. Research of carbon sink capacity caused by rock weathering process in China (in Chinese). Dissertation for the Doctoral Degree. Changsha: Central South University, 2003
29 Yin Y P. Karst development characteristics under the lithologic control of carbonate rocks—A case study in south-central Guizhou (in Chinese). Carsol Sin, 1994, 13: 31–36
30 Zhu Z. Discussion on influencing factors upon specific corrodibility and specific solubility of carbonate rock (in Chinese). Guangxi Geol, 1997, 10: 37–44
31 Weng J T. The Differential corrosion of calcites and dolomites (in Chinese). Carsol Sin, 1984, 29–38
32 Wei X G. Study on riverine carbon flux and erosion of Zhujiang (Pearl) River drainage basin in Chinese). Dissertation for the Doctoral Degree. Guiyang: Institute of Geochemistry, Chinese Academy of Sciences, 2003
33 Ferris F G, Wiese R G, Fyfe W S. Precipitation of carbonate minerals by microorganisms:Implications for silicate weathering and the global carbon dioxide budget. Geomicrobiol J, 1994, 12: 1–13
34 Liu Z H, Wolfgang D, Wang H J. A possible important CO_2 sink by the global water cycle. Chinese Sci Bull, 2007, 53: 402–407
35 Liu Z H, Wolfgang D, Wang H J. A new direction in effective accounting for the atmospheric CO_2 budget: Considering the combined action of carbonate corrosion, the global water cycle and photosynthetic uptake of DIC by aquatic organisms. Earth-Sci Rev, 2010, 99: 162–172